









# Intermittent Heating in the Magnetic Cloud Sheath Regions

Zilu Zhou<sup>1,2,3</sup> , Pingbing Zuo<sup>1</sup> , Fengsi Wei<sup>1,2</sup>, Xueshang Feng<sup>1,2</sup> , Yi Wang<sup>1</sup>, Ludi Wang<sup>1</sup>, Chaowei Jiang<sup>1</sup> ,  
Xiaojuan Song<sup>1,2,3</sup> , and Xiaojun Xu<sup>4</sup> 

<sup>1</sup> Laboratory for Space Weather Storms, Institute of Space Science and Applied Technology, Harbin Institute of Technology, Shenzhen, Shenzhen 518000, People's Republic of China; [pbzuo@hit.edu.cn](mailto:pbzuo@hit.edu.cn)

<sup>2</sup> SIGMA Weather Group, State Key Laboratory for Space Weather, National Space Science Center, Chinese Academy of Sciences, Beijing 100190, People's Republic of China

<sup>3</sup> University of Chinese Academy of Sciences, Beijing 100190, People's Republic of China

<sup>4</sup> State Key Laboratory of Lunar and Planetary Sciences, Macau University of Science and Technology, Macao, People's Republic of China

Received 2019 March 14; revised 2019 October 9; accepted 2019 October 9; published 2019 October 29

## Abstract

Coherent structures such as current sheets have been usually regarded to be sites of proton heating in the solar wind. In this Letter, we statistically investigate the proton heating effects around the coherent structures within the turbulent sheath regions of magnetic clouds (MCs) based on *WIND* observations. It is found that the proton temperature enhancement near coherent structures in the MC sheath is not as remarkable as in the solar wind. Significant temperature increase only exists near coherent structures with great directional changes ( $>45^\circ$ ) in magnetic field or intensity changes ( $\geq 10\%$  of the mean magnetic field magnitude), which merely account for 13% of the total of 12,426 identified intermittent events in the 71 studied MC sheaths. The temperature increment is more evident near strong current sheets with great directional changes ( $>45^\circ$ ) at smaller scales than those at larger scales. It suggests that the heating effects in the MC sheath regions are likely to be highly localized. The local proton heating effects in the turbulent sheath are probably caused by the magnetic reconnection processes that are frequently associated with the strong current sheets.

*Key words:* magnetic reconnection – solar wind – turbulence

## 1. Introduction

A well-known feature of solar wind turbulence is the occurrence of intermittency, that is, the distributions of field fluctuations at smaller scales will become non-Gaussian at a greater rate (Marsch & Tu 1997). The intermittency is generally associated with localized structures such as current sheets (Bruno & Carbone 2013; Matthaeus et al. 2015). These structures are ubiquitous in the solar wind and are used to be characterized as classical discontinuities (Burlaga 1968; Hudson 1970; Tsurutani & Smith 1979; Borovsky 2008). More recent studies indicated that current sheets may be coherent structures generated by magnetohydrodynamic (MHD) turbulence (Vasquez et al. 2007; Greco et al. 2008, 2009; Zhdankin et al. 2012; Zhang et al. 2015; Yang et al. 2017).

Current sheets in the solar wind have been suggested to be sites of enhanced dissipation (Burlaga 1968; Leamon et al. 2000). Osman et al. (2011) found that coherent structures are in statistical association with elevated proton temperatures, indicating that inhomogeneous heating linked to current sheets occurs in the solar wind. A subsequent study suggested that proton temperature increases locally at coherent structures and the temperature enhancement is more pronounced near stronger current sheets (Osman et al. 2012b). Dissipation and heating locally at turbulence-generated coherent structures are also observed in numerical simulations (Servidio et al. 2012; Wan et al. 2012, 2015). However, this issue has some controversial aspects. In a separate statistical study, Borovsky & Denton (2011) found no evidence for significant local heating of protons or electrons in strong current sheets.

It is worth noting that strong current sheets are usually associated with magnetic reconnection (Servidio et al. 2009, 2011; Osman et al. 2014). While turbulence commonly exists in space plasmas, the role of magnetic reconnection and

other possible dissipation mechanisms such as ion instabilities is not unambiguously known (e.g., Bale et al. 2009). Observational studies of magnetosheath turbulence suggested that magnetic reconnection in thin current sheets could facilitate the dissipation of magnetic energy at kinetic scales (Retinò et al. 2007; Sundkvist et al. 2007; Phan et al. 2018; Wilder et al. 2018; Stawarz et al. 2019). Such small-scale intermittent structures are prevalent in the Earth's magnetosheath and have been revealed to be sites for local dissipation using high-resolution data obtained by *Cluster* and *Magnetospheric Multiscale* missions (Chasapis et al. 2015, 2017, 2018; Chhiber et al. 2018). In the solar wind, magnetic reconnection is often related to the Petschek-like reconnection exhausts extending from the reconnection sites (Gosling et al. 2005). Reconnection exhausts have been observed frequently in the low- $\beta$  plasmas, but rarely in the compressed sheath regions in front of interplanetary coronal mass ejections (ICMEs; Phan et al. 2010; Gosling 2012). Therefore, studying the turbulence intermittency and its heating effects in the magnetic cloud (MC) sheath may shed some light on solar wind heating.

In this Letter, we will examine the proton temperature variation around intermittent structures in the sheath regions of 71 MC events observed by the *WIND* spacecraft to investigate the nature of intermittent heating in the MC sheath.

## 2. Data, Event List, and Method

The magnetic field and plasma data used to analyze the associated local heating of intermittent structures are obtained from the the Magnetic Field Investigation (MFI; Lepping et al. 1995) and the Three Dimensional Plasma analyzer (3DP; Lin et al. 1995) on board *WIND* spacecraft, respectively. The time resolutions are both 3 s. The lower-resolution magnetic field and plasma data obtained from MFI and the Solar Wind

Experiment (SWE; Ogilvie et al. 1995) are used to identify the MC sheaths.

The large-scale MCs (time duration greater than 12 hr) with unambiguous sheaths ahead are selected from a combined list with MC events identified based on a force-free magnetic field model (Lepping et al. 1990). The MCs identified from 1995 to 2012 are listed on the website<sup>5</sup> and the MC list from 2012 to 2015 can be found in the paper of Lepping et al. (2018). The exact time of shocks driven by the MCs can be found in the database of heliospheric shock waves maintained at University of Helsinki.<sup>6</sup> The MC sheath refers to the region between the leading shock and the MC's front boundary layer (BL). The BLs are identified according to the criteria of Wei et al. (2003). Since the plasmas are usually heated in the near downstream of MC-driven shocks and inside BLs, we exclude a 30 minute interval at either end of the sheath to eliminate the interference of the heating effects near the shocks and BLs. The time intervals of the sheaths studied in this Letter are listed in Table 1. The averaged bulk flow speed in the MC sheaths is  $498 \text{ km s}^{-1}$ . The averaged proton  $\beta$  is 0.64. The ion inertial length and ion gyroradius are 62 km and 49 km, respectively. The ratio of bulk velocity to Alfvén speed is larger than 4 in each MC sheath; thus, we consider the Taylor hypothesis to be roughly valid to relate the temporal scales to the spatial scales.

A normalized parameter named Partial Variance of Increments (PVI) has been widely used to identify intermittent structures in solar wind turbulence (Greco et al. 2008, 2018). The PVI value is computed as

$$\text{PVI} = \frac{|\Delta \mathbf{B}(t, \tau)|}{\sqrt{\langle |\Delta \mathbf{B}|^2 \rangle}}, \quad (1)$$

where  $\mathbf{B}$  is the magnetic field vector,  $|\Delta \mathbf{B}(t, \tau)| = |\mathbf{B}(t + \tau) - \mathbf{B}(t)|$ ,  $\tau$  is the time lag, and  $\langle \dots \rangle$  denotes an average over the entire data set of each MC sheath. In the solar wind, the most significant enhancements in proton temperature are associated with PVI events above a threshold of 3 (Osman et al. 2012a), which correspond to the intermittent current sheet structures (Greco et al. 2009). The same threshold of 3 is applied in this research for the identification of intermittent structures. Then a superposed-epoch analysis is applied to investigate the heating effects of the intermittent structures in the MC sheath. The proton temperature data with a time interval of 24 minutes at each side (leading and following) of the selected PVI events are extracted for this study. A normalized temperature conditioned on the distance from PVI events above the threshold of 3 is calculated as  $\langle T_p(r_l + \Delta r) / T_p(r_l) \rangle$ , where  $\Delta r$  is the spatial lag relative to the PVI events at  $r_l$ , and is calculated as  $\Delta r = V_{\text{sh}} \tau \approx 500 \tau$  km using Taylor's hypothesis.

### 3. Results

Figure 1 shows an MC observed by *WIND* on 2012 October 8. A fast shock passed the spacecraft at 04:12 UT, marked by the blue vertical line. The front BL is bounded by the two discontinuities (see the green vertical lines denoted " $M_f$ " and " $G_f$ " respectively). In the sheath region between the shock and " $M_f$ " both the plasma density and temperature are high, while

**Table 1**  
List of 71 Magnetic Cloud Sheaths Investigated in This Letter

| No. | Start             | End               |
|-----|-------------------|-------------------|
| 1   | 1995 Aug 22 13:26 | 1995 Aug 22 18:25 |
| 2   | 1995 Oct 18 11:11 | 1995 Oct 18 16:30 |
| 3   | 1997 Jan 10 01:22 | 1997 Jan 10 03:24 |
| 4   | 1997 Feb 9 13:20  | 1997 Feb 9 22:40  |
| 5   | 1997 May 15 01:45 | 1997 May 15 07:01 |
| 6   | 1997 Oct 10 16:27 | 1997 Oct 10 19:50 |
| 7   | 1997 Nov 22 09:42 | 1997 Nov 22 14:15 |
| 8   | 1998 Jan 6 13:59  | 1998 Jan 7 00:50  |
| 9   | 1998 Mar 4 11:32  | 1998 Mar 4 13:45  |
| 10  | 1998 May 1 21:51  | 1998 May 2 07:50  |
| 11  | 1998 Aug 19 19:10 | 1998 Aug 20 04:20 |
| 12  | 1998 Sep 24 23:50 | 1998 Sep 25 05:10 |
| 13  | 1998 Nov 8 05:11  | 1998 Nov 8 22:55  |
| 14  | 1999 Feb 18 03:18 | 1999 Feb 18 11:20 |
| 15  | 2000 Feb 20 21:33 | 2000 Feb 21 14:02 |
| 16  | 2000 Jun 23 13:28 | 2000 Jun 24 06:30 |
| 17  | 2000 Jul 28 10:31 | 2000 Jul 28 13:40 |
| 18  | 2000 Aug 11 19:19 | 2000 Aug 12 03:30 |
| 19  | 2000 Sep 17 17:18 | 2000 Sep 17 21:20 |
| 20  | 2000 Oct 3 01:32  | 2000 Oct 3 16:04  |
| 21  | 2000 Oct 12 23:03 | 2000 Oct 13 16:11 |
| 22  | 2000 Oct 28 10:00 | 2000 Oct 28 21:52 |
| 23  | 2000 Nov 6 09:59  | 2000 Nov 6 17:00  |
| 24  | 2001 Mar 19 12:03 | 2001 Mar 19 22:44 |
| 25  | 2001 Apr 11 16:47 | 2001 Apr 11 21:57 |
| 26  | 2001 Apr 21 15:59 | 2001 Apr 21 23:04 |
| 27  | 2001 Apr 28 05:30 | 2001 Apr 28 14:55 |
| 28  | 2001 May 27 15:15 | 2001 May 28 08:30 |
| 29  | 2001 Oct 31 14:16 | 2001 Oct 31 18:50 |
| 30  | 2002 Apr 17 11:31 | 2002 Apr 18 03:35 |
| 31  | 2002 May 18 20:15 | 2002 May 19 02:15 |
| 32  | 2002 May 23 11:14 | 2002 May 23 22:03 |
| 33  | 2002 Aug 1 23:39  | 2002 Aug 2 05:35  |
| 34  | 2002 Sep 30 08:24 | 2002 Sep 30 21:06 |
| 35  | 2004 Apr 3 15:21  | 2004 Apr 4 01:35  |
| 36  | 2004 Jul 24 06:00 | 2004 Jul 24 11:20 |
| 37  | 2004 Nov 7 18:29  | 2004 Nov 7 21:23  |
| 38  | 2005 May 15 02:43 | 2005 May 15 04:34 |
| 39  | 2005 Jun 12 07:18 | 2005 Jun 12 14:10 |
| 40  | 2005 Jun 14 18:25 | 2005 Jun 15 03:50 |
| 41  | 2005 Jul 17 01:22 | 2005 Jul 17 14:00 |
| 42  | 2007 Nov 19 17:52 | 2007 Nov 19 22:30 |
| 43  | 2009 Jun 27 11:34 | 2009 Jun 27 13:30 |
| 44  | 2010 Apr 5 08:26  | 2010 Apr 5 11:30  |
| 45  | 2010 May 28 02:23 | 2010 May 28 17:52 |
| 46  | 2010 Dec 19 21:05 | 2010 Dec 20 00:26 |
| 47  | 2011 Feb 18 01:19 | 2011 Feb 18 17:59 |
| 48  | 2011 Mar 29 15:39 | 2011 Mar 29 20:30 |
| 49  | 2011 Oct 5 07:16  | 2011 Oct 5 08:04  |
| 50  | 2011 Oct 24 18:09 | 2011 Oct 24 20:20 |
| 51  | 2012 Jun 16 21:14 | 2012 Jun 16 22:10 |
| 52  | 2012 Sep 30 22:48 | 2012 Sep 30 23:52 |
| 53  | 2012 Oct 8 04:42  | 2012 Oct 8 15:58  |
| 54  | 2012 Oct 31 14:58 | 2012 Oct 31 19:50 |
| 55  | 2012 Nov 12 22:42 | 2012 Nov 13 06:56 |
| 56  | 2012 Nov 23 21:21 | 2012 Nov 24 10:40 |
| 57  | 2013 Apr 13 22:43 | 2013 Apr 14 12:17 |
| 58  | 2013 Apr 30 09:22 | 2013 Apr 30 12:09 |
| 59  | 2013 Jun 27 14:21 | 2013 Jun 28 00:56 |
| 60  | 2013 Jul 9 20:41  | 2013 Jul 10 09:27 |
| 61  | 2013 Jul 12 17:13 | 2013 Jul 13 03:14 |
| 62  | 2013 Oct 2 01:45  | 2013 Oct 2 20:15  |
| 63  | 2013 Nov 30 20:45 | 2013 Dec 1 01:50  |
| 64  | 2014 Apr 20 10:50 | 2014 Apr 21 05:42 |

<sup>5</sup> [https://wind.gsfc.nasa.gov/mfi/mag\\_cloud\\_S1.html](https://wind.gsfc.nasa.gov/mfi/mag_cloud_S1.html)

<sup>6</sup> <http://ipshocks.fi>

**Table 1**  
(Continued)

| No. | Start             | End               |
|-----|-------------------|-------------------|
| 65  | 2014 Aug 19 06:18 | 2014 Aug 19 13:20 |
| 66  | 2014 Dec 21 19:08 | 2014 Dec 21 22:10 |
| 67  | 2015 Jan 7 06:09  | 2015 Jan 7 07:00  |
| 68  | 2015 Mar 17 04:30 | 2015 Mar 17 10:10 |
| 69  | 2015 May 6 01:25  | 2015 May 6 11:00  |
| 70  | 2015 Jul 13 01:35 | 2015 Jul 13 15:14 |
| 71  | 2015 Nov 6 18:15  | 2015 Nov 7 06:10  |

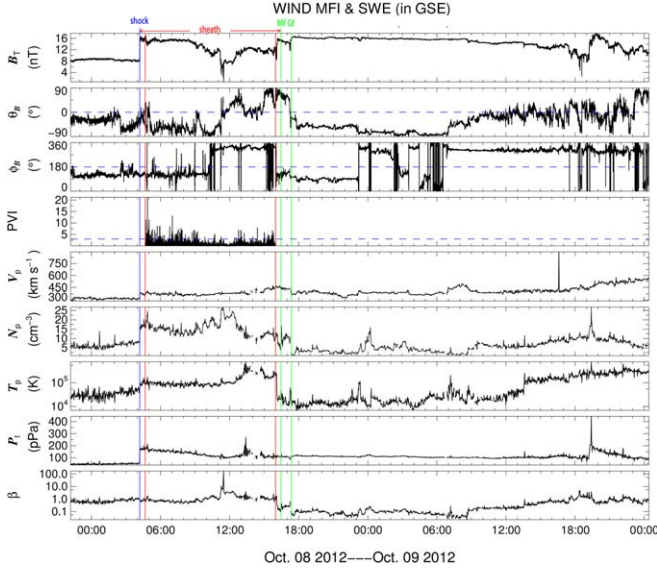


**Figure 1.** Magnetic cloud observed by *WIND* on 2012 October 8. A driven shock (blue vertical line) is located at 04:12 UT. The MCBL is bounded by the two discontinuities marked by the green lines. The sheath region investigated is bounded by the two red vertical lines.

the magnetic field is strong but turbulent. As mentioned above, we exclude a 30 minute interval at both ends of the sheath to eliminate the interference of the heating effects near the shock and BL. Thus, the region bounded by the two red lines is the sheath studied in practice. The fourth panel of Figure 1 presents the PVI values calculated from the magnetic field in the sheath. The spikes over the threshold (blue dashed lines) indicate the presence of intermittent structures.

The superposed-epoch analysis results of normalized proton temperature around intermittent structures with PVI values above the threshold of 3 are shown in Figure 2. The time lag  $\tau$  is chosen to be 3 s, which is in the inertial range. A total of 12,426 PVI events have been identified using the criterion of  $PVI \geq 3$ . The averaged proton temperature of all these intermittent structures is shown in Figure 2(a). Only a 3% enhancement of proton temperature can be found, indicating that the local heating effect associated with intermittent structures in the MC sheath is not significant, which is different from the observations in the solar wind (Osman et al. 2012b).

To reveal the reason for this difference, the intermittent structures are grouped according to the intensity and direction changes of magnetic field. The intensity changes are determined by a normalized parameter  $\delta|B|/B_0$ , where  $\delta|B| = |\mathbf{B}(t + \tau)| - |\mathbf{B}(t)|$  and  $B_0$  is the average of the

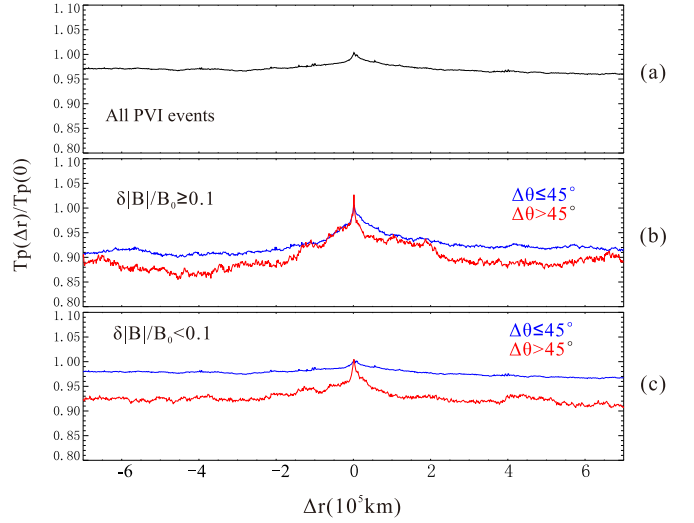


**Figure 2.** Superposed-epoch analysis of 12,426 intermittent events in the MC sheath identified using the criterion  $PVI \geq 3$ . The identified events are grouped into four categories: (1)  $\delta|B|/B_0 \geq 0.1$  and  $\Delta\theta > 45^\circ$ ; (2)  $\delta|B|/B_0 \geq 0.1$  and  $\Delta\theta \leq 45^\circ$ ; (3)  $\delta|B|/B_0 < 0.1$  and  $\Delta\theta > 45^\circ$ ; (4)  $\delta|B|/B_0 < 0.1$  and  $\Delta\theta \leq 45^\circ$ , where  $\delta|B| = |\mathbf{B}(t + \tau)| - |\mathbf{B}(t)|$ ,  $B_0$  is the averaged magnetic field intensity of the whole sheath, and  $\Delta\theta$  is the directional change. Averages of normalized proton temperature conditioned on the distance from (a) all events; (b) Group 1 (red line) and Group 2 (blue line) events; (c) Group 3 (red line) and Group 4 (blue line) events.

magnetic field strength of the whole sheath. The directional changes are also divided into two groups:  $\Delta\theta > 45^\circ$  and  $\Delta\theta \leq 45^\circ$ , as current sheets with  $\Delta\theta > 45^\circ$  are categorized to strong currents in Borovsky & Denton (2011). Thus, the intermittent structures are grouped into the following four categories: (1)  $\delta|B|/B_0 \geq 0.1$  and  $\Delta\theta > 45^\circ$ ; (2)  $\delta|B|/B_0 \geq 0.1$  and  $\Delta\theta \leq 45^\circ$ ; (3)  $\delta|B|/B_0 < 0.1$  and  $\Delta\theta > 45^\circ$ ; (4)  $\delta|B|/B_0 < 0.1$  and  $\Delta\theta \leq 45^\circ$ . Figure 2(b) shows the associated proton temperature of intermittent structures with significant magnetic field intensity changes ( $\delta|B|/B_0 \geq 0.1$ ). A substantial enhancement (10%) of the normalized proton temperature can be found regardless of the value of  $\Delta\theta$ , revealing that local heating is prominent near these coherent structures. Near the intermittent structures without large changes in magnetic field magnitude ( $\delta|B|/B_0 < 0.1$ ), local enhancement is still prominent (nearly 8%) near current sheets with large shear angles ( $\Delta\theta > 45^\circ$ ), but is not significant near current sheets with small shear angles ( $\Delta\theta \leq 45^\circ$ ), as shown in Figure 2(c). However, 10,831 of the total 12,426 intermittent structures identified fall into Group 4, so the average enhancement of normalized proton temperature is only 3%, as shown in Figure 2(a).

As shown in Figures 2(b) and (c), the normalized proton temperature suffers a significant enhancement near current sheets with  $\Delta\theta > 45^\circ$  (red lines). We then analyze the association between the temperature enhancement and the scale of such current sheets. The superposed-epoch analysis is performed for strong current sheets identified under four different time lags. Figure 3 shows that the temperature enhancement becomes more prominent as the spatial scale ( $\approx \tau \cdot V_{sh}$ ) of the current sheets decreases. Meanwhile, the heating effect is more localized near thinner current sheets. When the time lag is 3 s, the normalized proton temperature has already dropped 7% at a distance of  $10^5$  km, but it almost remains the same at this distance when the time lag increases to

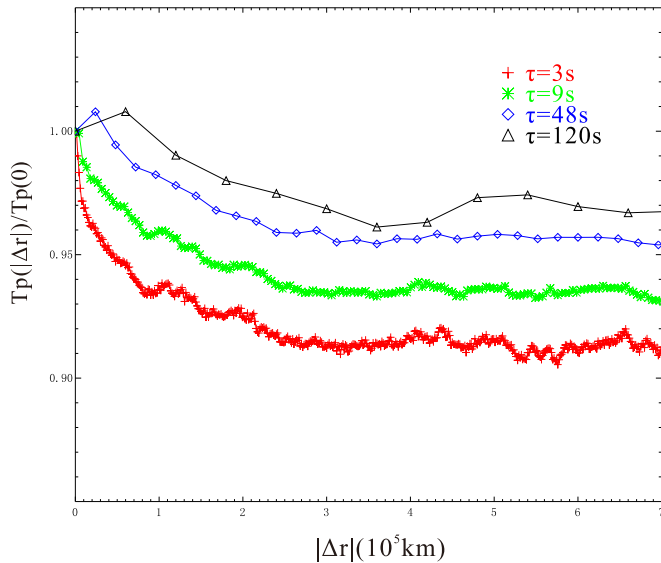


**Figure 3.** Averages of normalized proton temperature conditioned on the distance from strong current sheets ( $\Delta\theta > 45^\circ$ ) at different timescales.

120 s. This result suggests that the intermittent heating mainly occurs at thin current sheets instead of large-scale ones.

#### 4. Summary and Discussion

A total of 12,426 PVI events have been identified in the sheaths of 71 MC events observed by the *WIND* spacecraft, with the criterion of  $PVI \geq 3$ . Superposed-epoch analysis of normalized proton temperature associated with the PVI peaks identified shows that the averaged temperature enhancement is not prominent near the current sheets in the MC sheath, which is different from the results in the solar wind (Osman et al. 2012b). This motivates us to categorize the intermittent structures according to the magnitude and directional changes of the magnetic field. Strong current sheets, as characterized by  $\Delta\theta > 45^\circ$  in Borovsky & Denton (2011), turned out to be sites of proton heating. Additionally, temperature is substantially enhanced at intermittent structures with significant changes in magnetic field intensity. However, these structures are only a small fraction of the total of intermittent events identified. The averaged proton temperature increment is small near the weaker current sheets; thus, the averaged temperature enhancement of all intermittent events identified is not so prominent as in the solar wind.

The strong current sheets with large shear angles are candidate sites for magnetic reconnection (Servidio et al. 2009; Franci et al. 2017). Note that significant change in magnetic field magnitude during single-spacecraft crossing indicates a great gradient in field line linkage, which may lead to a breakdown of ideal MHD conditions and break the conservation of magnetic field topology (Priest & Démoulin 1995). It suggests that current sheets with significant changes in magnetic field intensity are also plausible reconnection sites. Therefore, our results suggest that prominent localized heating of protons can be found only at candidate reconnection sites, and the proportion of such sites would affect the averaged temperature in the superposed-epoch analysis for all intermittent structures. As the reconnection process is more prevalent in low- $\beta$  solar wind such as current sheets within ICMEs, the higher- $\beta$  sheath has a lower proportion of reconnection sites (Phan et al. 2010; Gosling 2012). Consequently, the temperature

enhancement is not so prominent in the MC sheath as in the solar wind.

The temperature enhancement is also found to be highly dependent on the scale of the strong current sheets. The temperature increment decreases as the thickness of the current sheets increases. This result may provide some clues to explain the contradictory results by Osman et al. (2012b) and Borovsky & Denton (2011). As seen in Figure 3, the enhancement at current sheets is weak at a time lag of 120 s, especially compared to the neighboring points. This may explain why the latter authors found no evidence for local heating at strong current sheets, as they compute the ratio of the proton temperature at current sheets to the averaged temperature of two adjacent points. The scale of reconnection sites in collisionless plasma is around the ion inertial length (Øieroset et al. 2001), which is about 100 km (less than 0.3 s, using Taylor’s hypothesis) in the solar wind and a bit smaller in the MC sheath. Since the highest resolution of plasma parameters obtained by *WIND* is only 3 s, it is difficult to capture the reconnection sites directly. Usually a spacecraft only encounters the reconnection exhausts far away from the reconnection sites. It is reasonable to suppose that thinner current sheet crossings are closer to the reconnection sites than thicker ones, and hence the temperature enhancement is more significant at thinner current sheets.

We thank the *WIND* MFI, SWE, and 3DP teams and CDAWeb for making available data used in this Letter. This work is jointly supported by the National Natural Science Foundation of China (41731067 and 41531073), 973 program (2012CB825601), Shenzhen Technology Project (JCYJ20170307150645407 and JCYJ20180306171748011), and the Specialized Research Fund for State Key Laboratories of China. Z.L.Z. thanks Dr. J. S. He for his helpful suggestions.

#### ORCID iDs

Zilu Zhou <https://orcid.org/0000-0002-4463-8407>  
 Pingbing Zuo <https://orcid.org/0000-0003-4711-0306>  
 Xueshang Feng <https://orcid.org/0000-0001-8605-2159>  
 Chaowei Jiang <https://orcid.org/0000-0002-7018-6862>  
 Xiaojian Song <https://orcid.org/0000-0002-7723-5743>  
 Xiaojun Xu <https://orcid.org/0000-0002-2309-0649>

#### References

- Bale, S. D., Kasper, J. C., Howes, G. G., et al. 2009, *PhRvL*, **103**, 211101  
 Borovsky, J. E. 2008, *JGRA*, **113**, A08110  
 Borovsky, J. E., & Denton, M. H. 2011, *ApJL*, **739**, L61  
 Bruno, R., & Carbone, V. 2013, *LRSF*, **10**, 2  
 Burlaga, L. F. 1968, *SoPh*, **4**, 67  
 Chasapis, A., Matthaeus, W. H., Parashar, T. N., et al. 2017, *ApJ*, **836**, 247  
 Chasapis, A., Matthaeus, W. H., Parashar, T. N., et al. 2018, *ApJL*, **856**, L19  
 Chasapis, A., Retinò, A., Sahraoui, F., et al. 2015, *ApJL*, **804**, L1  
 Chhiber, R., Chasapis, A., Bandyopadhyay, R., et al. 2018, *JGRA*, **123**, 9941  
 Franci, L., Cerri, S. S., Califano, F., et al. 2017, *ApJL*, **850**, L16  
 Gosling, J. T. 2012, *SSRv*, **172**, 187  
 Gosling, J. T., Skoug, R. M., McComas, D. J., & Smith, C. W. 2005, *JGRA*, **110**, A01107  
 Greco, A., Chuychai, P., Matthaeus, W. H., Servidio, S., & Dmitruk, P. 2008, *GeoRL*, **35**, L19111  
 Greco, A., Matthaeus, W. H., Perri, S., et al. 2018, *SSRv*, **214**, 1  
 Greco, A., Matthaeus, W. H., Servidio, S., Chuychai, P., & Dmitruk, P. 2009, *ApJL*, **691**, L111  
 Hudson, P. D. 1970, *P&SS*, **18**, 1611  
 Leamon, R. J., Matthaeus, W. H., Smith, C. W., et al. 2000, *ApJ*, **537**, 1054  
 Lepping, R. P., Acuña, M. H., Burlaga, L. F., et al. 1995, *SSRv*, **71**, 207

- Lepping, R. P., Jones, J. A., & Burlaga, L. F. 1990, *JGR*, **95**, 11957
- Lepping, R. P., Wu, C. C., Berdichevsky, D. B., & Szabo, A. 2018, *SoPh*, **293**, 65
- Lin, R. P., Anderson, K. A., Ashford, S., et al. 1995, *SSRv*, **71**, 125
- Marsch, E., & Tu, C. Y. 1997, *NPGeo*, **4**, 101
- Matthaeus, W. H., Wan, M., Servidio, S., et al. 2015, *RSPTA*, **373**, 20140154
- Ogilvie, K. W., Chornay, D. J., Fritzenreiter, R. J., et al. 1995, *SSRv*, **71**, 55
- Øieroset, M., Phan, T. D., Fujimoto, M., Lin, R. P., & Lepping, R. P. 2001, *Natur*, **412**, 414
- Osman, K. T., Matthaeus, W. H., Gosling, J. T., et al. 2014, *PhRvL*, **112**, 215002
- Osman, K. T., Matthaeus, W. H., Greco, A., & Servidio, S. 2011, *ApJL*, **727**, L11
- Osman, K. T., Matthaeus, W. H., Hnat, B., & Chapman, S. C. 2012a, *PhRvL*, **108**, 261103
- Osman, K. T., Matthaeus, W. H., Wan, M., & Rappazzo, A. F. 2012b, *PhRvL*, **108**, 261102
- Phan, T. D., Eastwood, J. P., Shay, M. A., et al. 2018, *Natur*, **557**, 202
- Phan, T. D., Gosling, J. T., Paschmann, G., et al. 2010, *ApJL*, **719**, L199
- Priest, E. R., & Démoulin, P. 1995, *JGR*, **100**, 23443
- Retinò, A., Sundkvist, D., Vaivads, A., et al. 2007, *NatPh*, **3**, 236
- Servidio, S., Greco, A., Matthaeus, W. H., Osman, K. T., & Dmitruk, P. 2011, *JGRA*, **116**, A09102
- Servidio, S., Matthaeus, W. H., Shay, M. A., Cassak, P. A., & Dmitruk, P. 2009, *PhRvL*, **102**, 115003
- Servidio, S., Valentini, F., Califano, F., & Veltri, P. 2012, *PhRvL*, **108**, 045001
- Stawarz, J. E., Eastwood, J. P., Phan, T. D., et al. 2019, *ApJL*, **877**, L37
- Sundkvist, D., Retinò, A., Vaivads, A., & Bale, S. D. 2007, *PhRvL*, **99**, 025004
- Tsurutani, B. T., & Smith, E. J. 1979, *JGR*, **84**, 2773
- Vasquez, B. J., Abramenko, V. I., Haggerty, D. K., & Smith, C. W. 2007, *JGR*, **112**, A11102
- Wan, M., Matthaeus, W. H., Karimabadi, H., et al. 2012, *PhRvL*, **109**, 195001
- Wan, M., Matthaeus, W. H., Roytershteyn, V., et al. 2015, *PhRvL*, **114**, 175002
- Wei, F., Liu, R., Fan, Q., & Feng, X. 2003, *JGRA*, **108**, 1263
- Wilder, F. D., Ergun, R. E., Burch, J. L., et al. 2018, *JGRA*, **123**, 6533
- Yang, L., Zhang, L., He, J., et al. 2017, *ApJ*, **851**, 121
- Zhang, L., He, J., Tu, C., et al. 2015, *ApJL*, **804**, L43
- Zhdankin, V., Boldyrev, S., Mason, J., & Perez, J. C. 2012, *PhRvL*, **108**, 175004